Multiscale Green's function for the deflection of graphene lattice

B. Yang*
Department of Mechanical and Aerospace Engineering, Florida Institute of Technology, Melbourne, Florida 32901, USA

V. K. Tewary
Materials Reliability Division, National Institute of Standards and Technology, Boulder, Colorado 80305, USA

(Received 11 January 2008; revised manuscript received 29 April 2008; published 27 June 2008)

We show analytically that the continuum limit of the lattice-statics Green's function of a graphene sheet corresponds to the Green's function for an elastically stable Kirchhoff plate but not the Green's function for two-dimensional Christoffel equations. This correspondence demonstrates the mechanical stability of graphene in deflection and is necessary for relating its mechanical parameters to its lattice parameters. An explicit expression is derived for relating the continuum flexural rigidity to the force constants of graphene. This relationship can be used to measure flexural rigidity of graphene directly from experimentally observed phonon dispersion curves. The flexural rigidity is predicted to be 0.797 eV by using the Tersoff–Brenner empirical potential. Numerical examples are presented to show the usefulness of the correspondence in bridging the lattice and continuum length scales in graphene.

DOI: 10.1103/PhysRevB.77.245442 PACS number(s): 62.25.−g, 62.20.D−, 63.20.−e

I. INTRODUCTION

Graphene is a two-dimensional (2D) hexagonal lattice of covalently bonded carbon atoms. It is regarded as one of the most exciting materials with a strong potential for application in powerful devices.[1,2] In order to develop graphene-based devices, a major challenge is to control/manipulate the curvature of graphene that is either suspended in a solution or laid on a substrate. This would require an understanding of the mechanical deflection of graphene and to develop techniques for its multiscale modeling, ranging from the atomistic to the device level. Recent observations of graphene ripples have sparked great interest in this problem.[3]

The deflection in graphene can be efficiently modeled by using the lattice Green's function (GF) at the atomistic level and the continuum GF at the macroscopic level, provided we can establish a correspondence between the lattice and the continuum GFs. Such a correspondence has been rigorously proved for normal three-dimensional (3D) solids[4] but not yet for graphene. The objective of this paper is to show analytically that this correspondence holds for the case of graphene and to analyze the fundamental deflection behavior of graphene in terms of its lattice and continuum GFs.

The correspondence between the lattice and the continuum model of graphene is needed to understand the observed stability[5] of a graphene sheet against deflection. It was previously believed that a 2D lattice would be unstable, and hence, would not exist in reality.[6,7] The present calculations show that the lattice GF for graphene in the continuum limit corresponds to the Kirchhoff plate model, which is known[8] to be stable. This correspondence is also useful for determining the mechanical parameters of graphene from its lattice parameters by using the standard methods of the lattice theory,[9] and is needed for integrating the lattice and the continuum GFs for multiscale modeling applications.[10–12] The GF-based multiscale modeling is a powerful technique for solving a variety of problems involving multiple length scales. Recently the GF method has been used to develop multiscale boundary conditions and has been applied to atomistic simulations in graphene and graphite.[13]

It can be rigorously proved (see, for example, Ref. 4) that the asymptotic limit of the lattice GF of a solid is the GF for the corresponding Christoffel equations for the continuum model. As shown in the next section, the asymptotic limit of the 2D lattice GF, in the general case, is $\ln(r)$ in the complex r space as $r\to\infty$, where r is the distance between the source and the field points. Its real part is $\ln(r)$ and its imaginary part is $\arctan(r_y/r_x)$, where the x and the y axes are assumed to be in the plane of the 2D solid. The real part corresponds to the plane strain and the imaginary part to the antiplane strain. Henceforth, in this paper we will refer to only the real part of the Green's function. This behavior agrees with the GF for the Christoffel equations in 2D (see, for example, Ref. 14). However, the 2D Christoffel equations correspond to a line force parallel to the z axis in a 3D continuum, such as the force field, due to a straight dislocation. The 2D Christoffel equations do not correspond to a point force in a 2D solid.

The difference between a line force in a 3D continuum and a point force in a 2D continuum arises due to the fact that the displacement field in the continuum model is a continuous and differentiable variable. The equations of elastic equilibrium depend upon all components of the strain field. The strain field is related to the derivatives of the displacement field. For the displacement field to be differentiable, it must be defined over a finite continuous range and not just at discrete points. In the case of a line force in a 3D continuum, the displacement field $\boldsymbol{u}$ is uniform in the z direction. This implies that $\partial u_i/\partial z$ ($i=x,y$, or z) and the corresponding strain field are zero. This reduces the equations of elastic equilibrium to only two space variables x and y, which are referred to as 2D Christoffel equations. These equations correspond to plane strain and the corresponding GF has a $\ln(r)$ behavior.[14]

On the other hand, in the case of a point force in a 2D solid, the dependence of the displacement field on the z coordinate has to be written in terms of the Dirac delta function $\delta(z)$ because the solid exists only on the plane at $z=0$. In this

case $\partial u_i/\partial z$ and the corresponding strain field at $z=0$ is the derivative of the delta function, which is undefined or formally infinite. An infinite strain implies that a 2D solid is mechanically unstable. This difficulty is avoided in the continuum model of a plate by assuming the plate to be of "vanishing" thickness that approaches zero only in the mathematical limit. The derivatives in the plate theory are evaluated before the limit of zero thickness is taken. This procedure makes the plate stable. This model of a plate is thus basically different than the line force in a continuum in which the displacement is uniform in the z direction. The continuum GF for the deflection of a Kirchhoff plate due to a point force varies as $r^2 \ln(r)$,[8] whereas the GF for a line force in a 3D continuum varies as $\ln(r)$.

To summarize, the problem is that the asymptotic limit of the lattice GF for a point force in a general 2D solid is the continuum GF for a line force in a 3D solid and not the point force in a 2D solid. An exact 2D solid, that is, a solid with physically zero thickness, would be unstable against deflections. A stable 2D solid has to be modeled as a plate of "vanishing" thickness but its GF does not correspond to the lattice GF of a general 2D solid. This situation is different than the general 3D solids in which the lattice GF corresponds exactly to the continuum GF.

In the present work, we resolve the above inconsistency by showing analytically that the continuum limit of the lattice GF in the special case of graphene in the deflection mode is indeed $r^2 \ln(r)$ and not $\ln(r)$. This unusual behavior of the GF arises because of the unusual phonon dispersion of graphene. In general, the phonon frequency in any solid (1D, 2D, or 3D) would vary linearly with k in the long-wavelength limit,[9] where k is the magnitude of the phonon wave vector $\boldsymbol{k}$. As shown in Sec. II, it is the linear k dependence of the phonon frequency in the long-wavelength limit that gives the $\ln(r)$ behavior in the asymptotic limit of a general 2D lattice. In the special case of graphene, the phonon frequency for the transverse modes polarized normal to the plane of graphene varies as k^2 (Ref 15 and 16) and not k. We show that the k^2 dependence of the phonon dispersion leads to the $r^2 \ln(r)$ behavior of the lattice GF in the asymptotic limit. This clearly establishes the correspondence between the lattice and the continuum GF for a plate. This is also consistent with the mechanical stability of graphene.[5]

In Sec. II, we derive an expression for the lattice GF for an infinite 2D solid and obtain a simple analytical expression for its asymptotic limit based on the Born von Karman model[9] for the graphene lattice[15] and the Tersoff–Brenner potential[17] for the interatomic interactions. This asymptotic limit establishes a linkage between the lattice and the continuum GFs, as needed for the GF-based multiscale modeling.[10–12] The mechanical properties of graphene are determined by its electronic configuration as well as its ionic interactions and lattice structure. We consider here only the ionic part and the lattice structure. In the adiabatic approximation, inherent in the Born von Karman model, the electronic energies can be added to the ionic energies. Of course the electrons also affect the ionic interactions. This part of the electronic contribution is phenomenologically included in the Tersoff–Brenner potential.[17]

We also derive an analytical formula for the flexural rigidity, D, of graphene in terms of the interatomic force constants. The flexural rigidity of a plate is a measure of its resistance to flexural deformation.[8] Using the Tersoff–Brenner empirical potential,[17] we obtain $D=0.797$ eV. In Sec. III, we present a multiscale model of the deflection of graphene by linking the discrete lattice model with the continuum boundary conditions. We examine the behavior of a clamped circular graphene sheet under a uniform force field, and analyze the difference between the values predicted by the lattice and the continuum models. Finally, we present conclusions in Sec. IV.

II. LATTICE STATICS GREEN'S FUNCTION OF A GRAPHENE SHEET

We consider a hexagonal 2D graphene lattice with crystallographic axes taken as the reference frame and one of the hexagonal vertices as the origin. The z axis is assumed to be normal to the plane of the lattice. The 2D primitive vectors of graphene lattice structure[15] are $(\sqrt{3},1)a$ and $(\sqrt{3},-1)a$, where $2a$ is the lattice constant. Graphene lattice has two atoms per unit cell, which we label by κ where $\kappa=A$ or B, respectively, for the atoms equivalent to that at the origin and that at $(2/\sqrt{3},0)a$. We label each unit cell by the index L. Thus $L\kappa$ denotes the atom κ in the unit cell L and $\boldsymbol{r}(L\kappa)$ denotes the position of the lattice site. We define the 3×3 force-constant matrices $\boldsymbol{\Phi}$ between pairs of atoms[9] as follows:

$$\boldsymbol{f}(L\kappa) = \sum_{L'\kappa'} \boldsymbol{\Phi}(L\kappa, L'\kappa')\boldsymbol{u}(L'\kappa') \tag{1}$$

where $\boldsymbol{f}$ and $\boldsymbol{u}$ denote the force and displacement vectors respectively for an atom. Although the lattice itself is 2D, the force-constant matrices, and the force and displacement vectors are 3D because it deforms in the 3D space. For this model, the matrix elements $\boldsymbol{\Phi}_{iz}=\boldsymbol{\Phi}_{zi}=0$, where $i=x$ or y. The zz elements are equal for all atoms in the same neighbor shell. In the Tersoff–Brenner potential each atom directly interacts with its first and second neighbors only. We denote $\boldsymbol{\Phi}_{zz}=\gamma$ for all the three nearest neighbors and δ for all the six second neighbors of the atom at the origin. The values of γ and δ are, respectively, 5.248 and -0.8747 eV/Å^2.

First, we calculate the lattice-statics GF (Ref. 4 and 9) for an infinite solid. We take the Fourier transform of the force-constant matrix, which is just the dynamical matrix multiplied by the atomic mass. This matrix is Hermitian 6×6 and is block diagonal. The 2×2 block matrix corresponding to z modes, that is, for displacements in the z direction, is denoted by $\boldsymbol{Z}(\boldsymbol{k})$. Its matrix elements, labeled by A and B, are given below:

$$Z_{AA}(\boldsymbol{k}) = Z_{BB}(\boldsymbol{k}) = 3\gamma + 6\delta - 2\delta[2\cos(\sqrt{3}k_x)\cos(k_y) + \cos(2k_y)], \tag{2}$$

$$Z_{AB}(\boldsymbol{k}) = -\gamma \exp\left(-\frac{\iota k_x}{\sqrt{3}}\right)[\exp(\iota\sqrt{3}k_x) + 2\cos(k_y)], \tag{3}$$

where $\iota=\sqrt{-1}$. The two eigenvalues of $\boldsymbol{Z}(\boldsymbol{k})$ are

$$\omega_{o,a}^2(\boldsymbol{k}) = Z_{AA}(\boldsymbol{k}) \pm \gamma[1 + 4\cos(\sqrt{3}k_x)\cos(k_y) + 4\cos^2(k_y)]^{1/2}, \tag{4}$$

where the plus and the negative signs give the optical and the acoustic mode frequencies ω_0 and ω_a, respectively. The lattice-statics GF (Ref. 4) for the deflection (z displacements) is given by

$$G(0\kappa, L\kappa') = \frac{1}{N}\sum_{\boldsymbol{k}} [Z^{-1}(\boldsymbol{k})]_{\kappa\kappa'} \exp\{\imath\boldsymbol{k}\cdot[\boldsymbol{r}(L\kappa') - \boldsymbol{r}(0\kappa)]\}, \tag{5}$$

where the sum is over all $\boldsymbol{k}$ vectors in the first Brillouin zone and N is the number of the $\boldsymbol{k}$ vectors. Since $\boldsymbol{Z}(\boldsymbol{k})$ is just a 2×2 matrix, the sum over $\boldsymbol{k}$ in Eq. (5) can be easily evaluated.

We now evaluate the asymptotic limit of G for large $|\boldsymbol{r}(L\kappa') - \boldsymbol{r}(0\kappa)|$ by using Duffin's lemma.[4] Since $\boldsymbol{Z}^{-1}(\boldsymbol{k})$ has poles at $k=0$, the asymptotic limit of the sum in Eq. (5) is obtained by expanding $\boldsymbol{Z}$ around $k=0$, treating $\boldsymbol{r}$ and $\boldsymbol{k}$ as continuous variables, and replacing the summation by an integral. The continuum model does not distinguish between sublattices and, in the acoustic modes, the two sublattices vibrate in phase. We, therefore, assume both κ and κ' in Eq. (5) to be type A and write $\boldsymbol{r}$ for $\boldsymbol{r}(LA)$. This gives the following from Eq. (5) in the asymptotic limit. $r\to\infty$:

$$G(0,\boldsymbol{r}) = \frac{1}{2V}\int \left[\frac{1}{E_a(k)} + \frac{1}{E_0(k)}\right]\exp(\imath\boldsymbol{k}\cdot\boldsymbol{r})d\boldsymbol{k}, \tag{6}$$

where the integration is over all k space and V is the area of the first Brillouin zone,

$$E_a(k) = (\gamma + 6\delta)k^2 - \frac{1}{12}(\gamma + 18\delta)k^4, \tag{7}$$

and

$$E_o(k) = 6\gamma - (\gamma + 6\delta)k^2 - \frac{1}{12}(\gamma + 18\delta)k^4. \tag{8}$$

Note that $E_a(k)$ and $E_o(k)$ are functions of k and do not depend upon the angle of $\boldsymbol{k}$. The GF, therefore, is isotropic, as expected for a hexagonal lattice. Since the $1/E_o(k)$ term in Eq. (6) does not have a pole at $k=0$, it does not contribute to the integral in the asymptotic limit. This is consistent with the continuum model, which does not include optical modes.

Both $E_a(k)$ and $E_o(k)$ are proportional to $\omega^2(k)$. The leading term in $E_a(k)$ in Eq. (7) as $k\to 0$ is k^2, which gives the linear dependence of the phonon frequencies on k in the continuum model. The integral of this term in Eq. (6) is proportional to $\ln(r)$ (see, for example, Ref. 14). Hence, for a general 2D solid, the asymptotic limit of the lattice GF varies as $\ln(r)$. As discussed in Sec. I, this corresponds to the continuum GF for a line force in a 3D solid and not to a point force in a 2D solid. This is the inconsistency described in Sec. I in the correspondence between the lattice and the continuum GF for 2D solids.

However, graphene is unusual because the coefficient $\gamma + 6\delta$ of the k^2 term in Eq. (7) is zero. Hence the leading term in the expansion of $E_a(k)$ for graphene in Eq. (7) is the k^4 term and not the k^2 term. This is not just an artifact of the Tersoff–Brenner potential. It is an inherent characteristic of the graphene lattice and has also been observed experimentally in graphite.[15,16] Thus, we obtain the following expression from Eqs. (6) and (7) for graphene:

$$G(0,\boldsymbol{r}) = -\frac{6}{V(\gamma + 18\delta)}\int \frac{\exp(\imath\boldsymbol{k}\cdot\boldsymbol{r})}{k^4}d\boldsymbol{k}. \tag{9}$$

The integration in Eq. (9) can be done analytically by differentiating under the integral sign with respect to x and y components of $\boldsymbol{r}$. This gives

$$G(0,r) = -\frac{3\sqrt{3}r^2\ln(r)}{2\pi(\gamma + 18\delta)a^2}, \tag{10}$$

where we have used $V = 2/\sqrt{3}\pi^2a^2$ for the area of the first Brillouin zone of graphene. Independently from above, the continuum GF for a Kirchhoff plate[8] is given by

$$G_K(0,r) = \frac{r^2\ln(r)}{8\pi D}, \tag{11}$$

where $D(\equiv EI)$ is the flexural rigidity of the plate. In the definition of the continuum flexural rigidity, E is the Young's modulus and I is the moment of inertia. Given in Ref. 8 is the point force solution of a finite circular plate. The above formula (11) can be derived by taking the plate radius to approach infinity and dropping the lower order terms.

We see from Eqs. (10) and (11) that $G(0,r)$ has exactly the same dependence on r as the GF for the Kirchhoff model. If the k^2 term in Eq. (7) were not zero as in the general case of a 2D solid, $G(0,r)$ would have a $\ln(r)$ behavior and not agree with the Kirchhoff model. Since the Kirchhoff plate is elastically stable, the correspondence between Eqs. (10) and (11) shows the stability of the graphene lattice in the elastic limit. Comparing Eqs. (10) and (11), we obtain

$$D = -\frac{\sqrt{3}}{36}(\gamma + 18\delta)a^2. \tag{12}$$

For the Tersoff–Brenner potential, $a = 1.2563$ Å, which gives $D = 0.797$ eV.

We see from Eq. (10) that the GF diverges with increasing r. The divergence at large r is associated with the singularity at $k=0$ in Eq. (6). Physically the divergence of the GF can be understood as follows: If one applies a vertical force at the center of a 2D solid of finite rigidity, the displacement will be zero at infinity and infinite at the center. Alternatively, when measured relative to the center, the displacement of the center will be zero and increase with distance, as predicted by Eq. (10), because of the lack of constraining forces.

III. MULTISCALE MODELING OF DEFLECTION OF A GRAPHENE LATTICE

Although Eq. (5) gives the lattice-statics GF for any atom, a direct real-space calculation is useful for modeling the mechanics of materials. The above derivation shows that the asymptotic behavior of the lattice-statics GF is the continuum plate GF. We exploit this correspondence in a cell

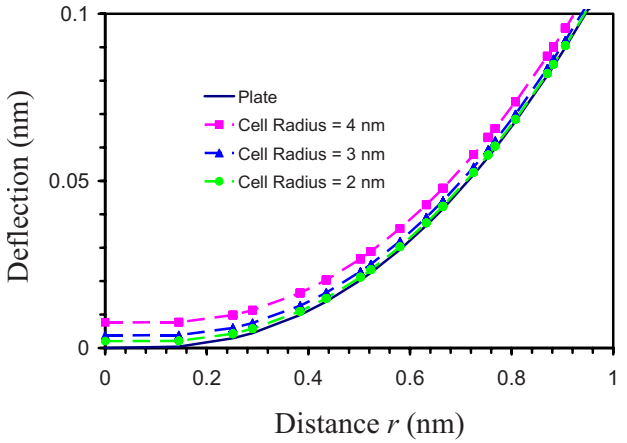

FIG. 1. (Color online) Variation of deflection with distance r due to a unit point force. The symbols indicate atoms.

model and show numerically the asymptotic approach in real space. A cell refers to a finite region of the solid containing discrete atoms. We calculate the GF and its derivative directly from Eq. (1) for cells of different radii and use the continuum plate GF (Ref. 8) as the boundary condition. The continuum GF boundary condition is imposed by assigning values of the continuum GF (i.e., physical displacement) to the atoms over the cell boundary. The atomic deflection and radial derivative for cells of radii 2, 3, and 4 nm are shown in Figs. 1 and 2, respectively. The derivative was computed by differentiating a continuous field interpolated with nearby atomic positions with base functions 1, r, and $r^2 \ln(r)$.

From Figs. 1 and 2, it can be seen that the deflection does not converge with cell size around the source point where the point force is applied. However, the radial derivative converges well with cell size. Since the (first-order) derivative converges well, the higher-order derivatives must also converge well. It can be seen that the converged radial derivative is different from the continuum counterpart in the vicinity of the source point. On the other hand, it asymptotically approaches the continuum plate GF at large r.

Since the low k behavior of the integrand in Eq. (6) reflects the long-range behavior in real space, the singularity at $k=0$ can be compensated by constraining the solid in real

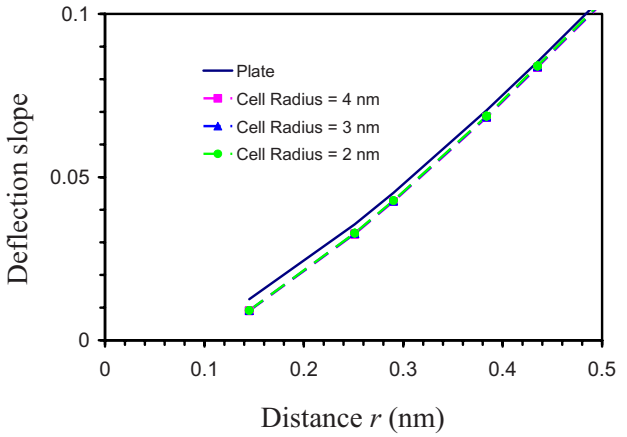

FIG. 2. (Color online) Variation of deflection slope with distance r due to a unit point force. The symbols indicate atoms.

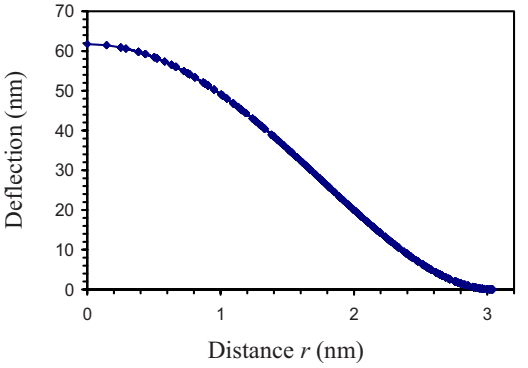

FIG. 3. (Color online) Variation of atomic deflection with distance r from central atom in a clamped circular graphene lattice subjected to a uniform force field. The symbols indicate atoms. The solid line is the continuum model result as predicted by Eq. (13).

space at large r. We consider a graphene sheet clamped over a circular boundary of radius r_0 under uniform pressure p. Under the clamped boundary condition (for all the atoms outside of the fixed circle), we solve Eq. (1) numerically for a force field of 1 eV/nm per atom and a (nominal) radius of 3 nm. The calculated atomic deflections are plotted against distance r from the central atom in Fig. 3. It can be seen that all the atoms fall on a single curve, consistent with the transverse isotropy of a hexagonal lattice.

We compare the lattice theory result given in Fig. 3 with that predicted by the continuum model. The classical solution of the deflection of a clamped circular Kirchhoff plate under a uniform pressure p is given by[8]

$$w = \frac{p r_0^4}{64D}\left[1 - \left(\frac{r}{r_0}\right)^2\right]^2. \tag{13}$$

In the present case $p=36.579$ eV/nm^3, corresponding to 1 eV/nm per atom force applied on the graphene lattice. Since the outer boundary of the lattice is zigzag, whereas for a Kirchhoff plate it is exactly a circle, the effective value of r_0 in Eq. (13) is different than that used in the lattice theory. We find an excellent fit between the lattice and the continuum theory results that offers the same flexural rigidity $D=0.797$ eV as analytically predicted in the previous section, and $r_0=3.13$ nm, which is close to 3 nm, the value chosen for the lattice calculation. This result is interesting because it shows that by choosing an effective value of r_0, the ordinary plate solution can be a very good approximation for the exact lattice-statics solution.

IV. CONCLUSIONS

We have analyzed the fundamental deflection behavior of a graphene lattice. We have derived an analytic expression for the zz component of the lattice GF of graphene and its asymptotic limit that agrees with the 2D continuum GF of a Kirchhoff plate. This correspondence shows the elastic stability of graphene in the continuum limit and can be used for relating its mechanical parameters to its discrete lattice parameters. It would also be useful for the multiscale modeling of graphene. Using the force constants derived from the

Tersoff–Brenner potential, the value of the flexural rigidity of graphene is found to be 0.797 eV. We have also shown that the flexural rigidity of graphene is directly related to the coefficient of the k^4 term in the phonon dispersion of the acoustic mode. Since the phonon dispersion can be measured [see, for example, Ref. 16] from which the coefficient of the k^4 term can be obtained, our formulation provides a direct method for measuring the flexural rigidity of graphene. In addition to the analytical results, we have presented a cell model for calculating the lattice-statics GF directly in real space using the continuum GF as a boundary condition. Finally, we have shown that a clamped graphene lattice under a uniform pressure behaves closely like an isotropic Kirchhoff plate.

ACKNOWLEDGMENTS

B.Y. acknowledges financial support from the National Science Foundation (Contract No. CMMI-0723486) and from the National Institute of Standards and Technology that initiated the work.

*Fax: 321-674-8813. boyang@fit.edu

[1] A. K. Geim and K. S. Novoselov, Nat. Mater. **6**, 183 (2007).
[2] M. I. Katsnelson, Mater. Today **10**, 20 (2007).
[3] S. V. Morozov, K. S. Novoselov, M. I. Katsnelson, F. Schedin, L. A. Ponomarenko, D. Jiang, and A. K. Geim, Phys. Rev. Lett. **97**, 016801 (2006).
[4] V. K. Tewary, Adv. Phys. **22**, 757 (1973).
[5] K. S. Novoselov, A. K. Geim, S. V. Morozov, D. Jiang, Y. Zhang, S. V. Dubonos, I. V. Grigorieva, and A. A. Firsov, Science **306**, 666 (2004).
[6] R. E. Peierls, Ann. Inst. Henri Poincare **5**, 177 (1935).
[7] L. D. Landau, Phys. Z. Sowjetunion **11**, 26 (1937).
[8] S. Timoshenko and S. Woinowsky-Krieger, *Theory of Plates and Shells* (McGraw-Hill, London, 1959).
[9] A. A. Maradudin, E. W. Montroll, G. H. Weiss, and I. P. Ipatova, in *Theory of Lattice Dynamics in the Harmonic Approximation*, Solid State Physics Supp. 3, 2nd ed., edited by H. Ehrenreich, F. Seitz, and D. Turnbull (Academic, New York, 1971).
[10] V. K. Tewary, Phys. Rev. B **69**, 094109 (2004).
[11] B. Yang and V. K. Tewary, Phys. Rev. B **75**, 144103 (2007).
[12] D. T. Read and V. K. Tewary, Nanotechnology, **18**, 105402 (2007).
[13] S. N. Medyanik, E. G. Karpov, and W. K. Liu, J. Comput. Phys. **218**, 836 (2006).
[14] V. K. Tewary, R. H. Wagoner, and J. P. Hirth, J. Mater. Res. **4**, 113 (1989).
[15] R. Saito, G. Dresselhaus, and M. S. Dresselhaus, *Physical Properties of Carbon Nanotubes* (Imperial College, London, 2003).
[16] L. Wirtz and A. Rubio, Solid State Commun. **131**, 141 (2004).
[17] D. W. Brenner, Phys. Rev. B **42**, 9458 (1990).